

THE ACTIVITY OF THE VINCULIN BINDING SITES IN TALIN IS INFLUENCED BY THE STABILITY OF THE HELICAL BUNDLES THAT MAKE UP THE TALIN ROD

B.C. Patel*, A.R. Gingras*, A.A. Bobkov[¶], L.M. Fujimoto[¶], M. Zhang[¶], R.C. Liddington[¶], D. Mazzeo*, J. Emsley[§], G.C.K. Roberts*, I.L. Barsukov* and D.R. Critchley*.

From the *Department of Biochemistry, University of Leicester, U.K., [¶]The Burnham Institute, 10901 North Torrey Pines Rd, La Jolla, CA 92037, USA, [§]School of Pharmacy, Centre for Biomolecular Sciences, University of Nottingham, Nottingham, NG7 2RD, U.K.

Running Title: Stability of helical bundles in the talin rod affects vinculin binding

Address correspondence to: David R. Critchley, Department of Biochemistry, University of Leicester, University Road, Leicester, LE1 7RH, UK, Tel.: (0)116 252 3477, Fax: (0) 116 252 5097, E-mail: drc@le.ac.uk

The talin rod contains ~11 vinculin binding sites (VBS's) each defined by hydrophobic residues in a series of amphipathic helices that are normally buried within the helical bundles that make up the rod. Consistent with this, talin failed to compete for binding of the vinculin Vd1 domain to an immobilised talin polypeptide containing a constitutively active VBS. However, talin did bind to GST-Vd1 in pull-down assays, and ITC measurements indicate a K_d of ~9 μ M. Interestingly, Vd1 binding exposed a trypsin-cleavage site in the talin rod between residues 898/899, indicating that there are one or more active VBS's in the N-terminal part of the talin rod. This region comprises a five helix bundle (residues 482-655) followed by a seven helix bundle (656-889), and contains five VBS's (helices 4, 6, 9, 11 and 12). The single VBS within 482-655 is cryptic at room temperature. In contrast, talin 482-889 binds Vd1 with high affinity (K_d ~ 0.14 μ M), indicating that one or more of the four VBS's within 656-889 are active, and this likely represents the vinculin-binding region in intact talin. In support of this, HA-tagged talin 482-889 localised efficiently to focal adhesions whereas 482-655 did not. Differential scanning calorimetry showed a strong negative correlation between Vd1 binding and helical bundle stability, and a 755-889 mutant with a more stable fold bound Vd1 much less well than wild-type. We conclude that the stability of the helical bundles that make up the talin rod is an important factor determining the activity of the individual VBS's.

The cytoskeletal protein talin is one of a number of proteins including filamin (1), α -actinin (2), tensin (3,4), and ILK (5) implicated in coupling integrins to F-actin in cellular junctions with the extracellular matrix (ECM). Talin was

originally described as a protein localised in cell-ECM junctions (focal adhesions; FAs) and membrane ruffles in cultured cells (6), and was subsequently shown to bind integrins in gel filtration studies (7). Its role as a key component of FAs is supported by antibody microinjection experiments (8,9), laser ablation studies (10), antisense RNA down-regulation (11), and *Tln* gene disruption studies in cells in culture (12-14). Knockout studies in mouse (15), *Drosophila* (16) and *C. elegans* (17) confirm that talin is essential for a wide spectrum of integrin-mediated developmental events including gastrulation in the mouse (15), though the situation is complicated by the discovery of a second talin gene (*Tln2*) in mammals (18).

Talin is an elongated (~60 nm) flexible protein (19), reportedly an anti-parallel dimer (20). The globular N-terminal talin head contains a FERM domain (residues 86-400) with binding sites for the cytoplasmic domains of the integrin β -subunit (21,22) and also layilin (a hyaluronan receptor) (23), F-actin (24), and two signalling proteins, FAK (23) and the type 1 γ 661 isoform of PI4'5'-kinase (25-29), both of which are implicated in regulating FA dynamics. The talin rod which is responsible for dimer formation (30), contains a conserved C-terminal actin-binding site (31), a second integrin-binding site (32), and several binding sites for the cytoskeletal protein vinculin (33), which itself has multiple binding partners including F-actin (34). Integrin signalling via FAK / Src promotes binding of talin to PIP-kinase (26). This activates PIP-kinase, and results in translocation of the talin / PIP-kinase complex to the plasma membrane (25). PIP2 has been shown to activate the integrin binding site(s) in talin (35), and the talin head has in turn been shown to activate integrins (36,37), suggesting a model in which the localised production of PIP2 drives the assembly of integrin/talin/F-actin

complexes (38) competent to engage the ECM. Recruitment of additional components might then facilitate the stabilisation and maturation of these complexes into FAs.

One protein that has been implicated in stabilising FAs is vinculin. Down-regulation of vinculin leads to smaller FAs and enhances cell motility (39), whereas overexpression of vinculin leads to larger FAs and suppresses motility (40). Studies on vinculin knockout cells are consistent with this data (41-44). Moreover, vinculin is recruited to FAs in response to applied mechanical force supporting the view that it plays a role in stabilising these structures (45). Using SDS-PAGE blot assays (46) and yeast two hybrid deletion mutants analysis (33,47), we previously identified three vinculin binding sites (VBS's) in the talin rod each defined by a single amphipathic helix. More recent data using synthetic peptides equivalent to each of the predicted 62 helices that make up the talin rod (48) indicate that there are at least 8 additional VBS's (49). Crystal structures show that the hydrophobic groups on one face of a talin VBS helix become embedded in a hydrophobic groove in the vinculin head (50-52), but our recent structural studies (52,53) show that these vinculin-binding determinants in talin are normally buried in the core of a series of amphipathic helical bundles that make up the talin rod (48). In the present study, we have sought to establish whether some or all of the VBS's in the talin rod are cryptic or constitutively active.

MATERIALS AND METHODS

Protein expression and purification-cDNAs encoding mouse talin 482-636, 482-655, 482-789, 755-889 and the chicken vinculin Vd1 domain (residues 1-258) were cloned into the expression vector pET-15b (Novagen, Cambridge Bioscience, Cambridge) whilst a cDNA encoding mouse talin 482-889 was cloned into pET-151/D-TOPO (Invitrogen). Recombinant proteins were purified as described previously (52,53), and protein concentrations determined using the CB-Protein Assay (Calbiochem).

cDNAs encoding human talin1 (residues 1-2541) and the talin1 rod domain (residues 453-2541) were generated by PCR using pET30a constructs encoding the N-terminal talin head and the talin rod as templates (kindly provided by Dr. Stephen C-T. Lam, University of Illinois, Chicago, Illinois). PCR products were cloned into pET30a

(Novagen) between the NdeI and EagI sites such that the encoded proteins were expressed with a C-terminal His tag. Constructs were authenticated by DNA sequencing and shown to match the human talin 1 cDNA sequence in GenBank (accession BC042923). Human talin1 and the talin1 rod were expressed in *E. coli* BL21(DE3). In brief, cells (1 litre) were grown at 37°C to an OD_{600nm} 0.6, and induced with 0.2mM isopropyl 1-thio-D-galactopyranoside at 15°C overnight. The cell pellet was resuspended into 35ml lysis buffer (20mM Tris, pH7.4, 0.4M NaCl) with 1mM β-mercaptoethanol, and lysed by passing through a French Press (Thermo Electron). The soluble cell lysate was then recovered and passed through a 5ml HiTrap affinity column (Amersham Bioscience) charged with Ni²⁺. Fractions containing the required protein were combined, concentrated and further purified by size exclusion chromatography (Superdex 200 10/30, Amersham Bio-sciences) in buffer containing 20 mM sodium phosphate (pH7.5), 150 mM NaCl and 0.1mM EDTA. The relationship of the various talin polypeptides used in this study to full-length talin is illustrated in Fig 1.

Binding of the vinculin Vd1 domain to talin- The relative affinities of talin and talin polypeptides for the vinculin Vd1 domain was measured by competitive ELISA as described previously (52). In brief, NUNC immunoplates (F96-maxisorp) coated with a talin 482-636 polypeptide were incubated with the GST-vinculin Vd1 domain at a concentration of 5nM (54) in the presence of increasing amounts of talin or recombinant talin polypeptides. Binding of GST-vinculin or GST alone was determined using a rabbit polyclonal anti-GST coupled to HRP (Santa Cruz). Binding of talin to GST-Vd1 was also measured using a pull down assay as described previously (47). Analytical gel filtration chromatography of recombinant talin polypeptides and vinculin Vd1 (1-258) was performed using Superdex-75 (10/30) (Pharmacia) at room temperature. The column was pre-equilibrated and run in 20 mM Tris (pH 8.0), 200 mM NaCl and 2 mM DTT at a flow rate of 0.8 ml/min. In each case, 0.5 ml fractions were collected and analysed using a 15% SDS-PAGE gel and stained using the GelCode blue reagent (Pierce).

Calorimetry-Differential scanning calorimetry (DSC) experiments were performed on a N-DSC II differential scanning calorimeter (Calorimetry Sciences Corp, Provo, UT) at the scanning rate of

1 K/min under 3.0 atm of pressure. Prior to measurement, protein samples were dialyzed against PBS. The dialysis buffer was used as the reference solution. Vd1 and talin polypeptides were used at concentrations between 18.0 and 25 μ M. Isothermal titration calorimetry (ITC) was performed on a VP-ITC calorimeter from Microcal (Northampton, MA). 8 μ l aliquots of solution containing 0.8 to 1.0 mM of vinculin Vd1 (residues 1-258) were injected into the cell containing 40 to 100 μ M talin or the talin polypeptide. In each experiment 37 injections were made. The experiments were performed at 23°C. Prior to ITC titrations, all protein samples were dialyzed against PBS buffer. Experimental data were analyzed using Microcal Origin software provided by the ITC manufacturer (Microcal, Northampton, MA).

Circular dichroism spectroscopy-CD spectra were recorded using a JASCO J-715 spectropolarimeter equipped with a JASCO PTC-348WI temperature control unit. Far-UV CD spectra were recorded at 20°C over the wavelength range 200-250 nm in a quartz cell of 0.1 cm path length (scan rate 50 nm \cdot min⁻¹). Proteins were dissolved in 20 mM sodium phosphate (pH 6.5), 50 mM NaCl at a concentration 25 μ M. The mean residue molar ellipticity $[\theta]$ (deg \times cm² \times dmol⁻¹) was calculated according to the formula: $[\theta] = \theta / (n \times 10 \times C_M \times l)$ where θ is the measured ellipticity in degrees, n is the number of peptide bonds (residue), l is the path length in centimeters and C_M is the molar protein concentration. The factor 10 originates from the conversion of the molar concentration to the dmol cm⁻³ concentration unit. For urea denaturation studies, proteins were dissolved in 20 mM sodium phosphate, pH 6.5, 50 mM NaCl containing 0, 0.8, 1.6, 4.0, or 5.6 M urea.

Expression of HA-tagged talin polypeptides in NIH3T3 cells-cDNAs encoding C-terminal HA-tagged talin polypeptides 482-636, 482-655, 482-789 and 482-889 were synthesized by PCR using the mouse talin-1 cDNA (55) as template, and the following primers from Invitrogen:

482, 5'-CGGGATCCATGCGAGGACACATGCC ACCT-3';

636, 5'-GGAATTCTCAAAGAGCGTAATCTGG AACATCGTATGGGTAGTTCTGACGAG-3';

655, 5'-GGAATTCTCAAAGAGCGTAATCTGG AACATCGTATGGGTAAATTTGCTGCAACA GCTC-3';

789, 5'-GGAATTCTCAAAGAGCGTAATCTG

GAACATCGTATGGGTAGGCGTGGGCCTTC ACGTG-3';

889, 5'- GGAATTCTCAAAGAGCGTAATCTG GAACATCGTATGGGTATCGCTGCTGCTGTT CCTC-3'.

PCR products were first cloned into pPCR-Script Amp SK(+) (Stratagene) and then subcloned into the expression vector pcDNA3 (Invitrogen) using BamHI and EcoRI sites. The authenticity of the cloned cDNAs were confirmed by sequencing. The constructs were transfected - 2 μ g cDNA / 6 μ l FuGENE 6 (Roche) - into 3×10^4 NIH 3T3 cells grown on glass coverslips and cultured in DMEM / 10% fetal bovine serum. After 16 h at 37°C, cells were fixed for 10 min in 4% paraformaldehyde/PBS, permeabilised for 5 min in 0.2% (v/v) Triton X-100/PBS and quenched for 10 min in 50 mM NH₄Cl/PBS. After 1 h incubation in 1% BSA/PBS, cells were incubated for 20 min with the anti-HA antibody (Santa Cruz Biotechnologies), washed three times with 0.02% BSA/PBS, and then incubated for 20 min with FITC-conjugated secondary antibody (Southern Biotechnology Associates, Inc.). F-actin was visualised by staining with phalloidin-Texas Red (Molecular Probes) for 20 min. Following three washes in 0.02% BSA/PBS, coverslips were mounted on glass slides using Prolong Antifade Reagent (Molecular Probes) and inspected using a Nikon TE300 inverted microscope and Openlab 4.0.2 software.

RESULTS

The vinculin-binding sites (VBS's) in talin are in a low affinity state-Our recent biochemical (33,47) and structural studies (52,53) show that the ~11 vinculin-binding sites (VBS's) in the talin rod (49) (Fig 1) are each contained within a single amphipathic helix. Binding is determined by a series of hydrophobic residues on one face of the helix, but these are normally buried in the core of the helical bundles that make up the talin rod (52,53). To investigate whether any of the VBS's in intact talin are active, we set up a competitive ELISA-type assay. Because the talin-binding site in the N-terminal region of vinculin is normally masked by an intramolecular interaction with the C-terminal vinculin tail (54,56), we used a GST-vinculin fusion protein containing just residues 1-258 (GST-Vd1) to assay talin binding. Similarly, since the single VBS contained within the N-terminal region the talin rod (residues 482-655, a

5-helix bundle) is cryptic (52), we used a construct (residues 482-636) in which the VBS has been activated by deletion of the C-terminal helix. We then measured the ability of GST-Vd1 to bind to talin 482-636 deposited on plastic in the presence of increasing concentrations of talin or talin fragments. As shown previously (52), preincubation of GST-Vd1 with increasing concentrations of talin 482-636 in solution progressively inhibited binding to talin 482-636 on plastic, with an IC_{50} of ~ 1 nM, whilst talin 482-655 was completely without effect (Fig 2A). Interestingly, talin purified from turkey gizzard was also unable to inhibit GST-Vd1 binding indicating that the VBS's in intact talin are cryptic or in a low affinity state (Fig 2A). The integrin-binding sites in talin are also reportedly cryptic, and can be activated by PIP2 (35), or by cleavage of the talin head from the rod (57). Preincubation of talin with PIP2 did not activate the VBS's in talin (Fig 2A), although the purified talin rod (but not the head) did show significantly more Vd1-binding activity than intact talin (Fig 2A).

The above assay provides a measure of the relative affinities of Vd1 for talin and talin fragments, and does not necessarily indicate that intact talin cannot bind vinculin. To investigate this, we incubated purified talin with GST or GST-Vd1 and carried out a pull down assay. Talin binding was analysed by SDS-PAGE followed by Western blotting using the TD77 monoclonal antibody that recognises the extreme C-terminus of talin (8). The results clearly establish that talin and talin rod fragments are able to bind to GST-Vd1 (Fig 2B). To obtain a direct measure of the binding affinities we used ITC (Table 1). At 23°C, Vd1 bound talin with a K_d of ~ 9 μ M, and PIP2 had relatively little effect on binding ($K_d \sim 5$ μ M). The talin rod bound Vd1 with a slightly higher affinity ($K_d = 2.4$ μ M) whereas Vd1 bound the short talin 482-636 polypeptide with a 30 fold higher affinity ($K_d = 0.3$ μ M) than intact talin. As expected, no binding could be detected to talin 482-655. The results are in good agreement with the semi-quantitative ELISA data and confirm that although intact talin can bind to vinculin, the interaction is of low affinity. Thus, talin is unable inhibit binding of Vd1 to talin 482-636 because the latter polypeptide binds Vd1 with much higher affinity.

Binding of vinculin Vd1 to intact talin exposes proteases cleavage sites in the talin rod-The affinity of Vd1 for talin suggests that the majority

of the ~ 11 VBS's in talin are cryptic and must be regulated in some way. We therefore sought an assay that might identify the approximate location of any active VBS's in the talin rod. Binding of Vd1 to a recombinant talin 755-889 (which contains 3 VBS's) induces a marked conformational change in the talin polypeptide that can be readily demonstrated by NMR, and also by an increase in sensitivity to proteolytic cleavage (53). We therefore explored the possibility that Vd1 binding to intact talin might expose previously buried trypsin cleavage sites that would indicate where Vd1 binding had occurred. Incubation of talin alone with trypsin liberated a protease-resistant 170 kDa fragment (Fig 3A) detected by monoclonal antibody 8D4 (epitope residues 482-655) (Fig 3B), but lacking the epitope for monoclonal antibody TD77 (residues 2494-2541) (Fig 3C). Consideration of the size of the fragment and the antibody data indicates that trypsin cleaves off the talin head liberating a rod fragment starting at about residue 482 which lacks the extreme C-terminal region of the rod. When intact talin was preincubated with Vd1, the ~ 170 kDa fragment was further cleaved to a ~ 140 kDa protease-resistant fragment (Fig 2A) which lacked the epitope for 8d4 (Fig 3B) as well as that for TD77 (Fig 3C). N-terminal sequencing showed that the ~ 140 kDa fragment starts at residue 899. Interestingly, the N-terminal region cleaved from the talin rod does not accumulate as a Coomassie blue positive band indicating that it is unstable. However, a series of 8d4 positive bands can be detected by Western blotting (Fig 3B). The results show that Vd1 binding to intact talin markedly effects the conformation of the N-terminal region of the talin rod (residues 482-898) rendering it protease sensitive, and indicating that this region must contain at least one active VBS.

Talin residues 656-889 contain one or more active VBS's-We have recently determined the structures of several polypeptides spanning the N-terminal part of the talin rod (52,53), and this has allowed us to propose a model (53) for the structure of residues 482-889 comprising a 5 helix bundle (residues 482-655; domain 1) followed by a 7 helix bundle (residues 656-889; domain 2) (53). Moreover, using synthetic peptides corresponding to each of the α -helices, we have shown that helices 4, 6, 9, 11 and 12 bind Vd1 (49) (Fig 1). To establish which if any of these VBS's are active, we analysed the ability of various talin polypeptides spanning this region to bind Vd1 in

both competitive ELISA and gel filtration assays. In the ELISA, talin 482-889 showed the highest affinity for GST-Vd1, and was even more effective at inhibiting binding of GST-Vd1 to immobilised talin 482-636 than soluble 482-636 itself (Fig 4). These results are consistent with ITC data which show that at 23°C, talin 482-889 binds Vd1 with a K_d of 0.14 μ M compared with a K_d of 0.3 μ M for talin 482-636 (Table 1). Since the single VBS (helix 4) in the 5 helix bundle is cryptic, we conclude that one or more of the four VBS's in the 7 helix bundle (domain 2) are able to bind Vd1 with high affinity. The talin 482-889 polypeptide also showed high affinity binding to Vd1 in gel filtration experiments, and at molar ratio of ~1:1, the proteins formed a complex with no unbound Vd1 remaining (Fig 5A). Progressive increases in the molar ratio of talin 482-889/Vd1 suggests that this talin polypeptide can bind up to three molecules of Vd1 (at a molar ration of 1:3, some free Vd1 was again detected).

Binding of Vd1 to talin 482-655 is inhibited by the stability of the 5-helix bundle-One of the factors that might influence the activity of a VBS is the inherent stability of the talin helical bundle in which it is embedded. To explore this possibility, we expressed various talin rod constructs containing VBS's, and used differential scanning calorimetry (DSC) to compare their stability with their ability to bind Vd1. As observed previously (54), a DSC scan shows that Vd1 has a rather broad melting profile and relatively low melting temperature (T_{m1} ~49°C and T_{m2} ~58°C), but becomes more ordered upon binding to the talin rod, resulting in the appearance of a sharp peak with a T_m of 66.0°C (Fig 6A). A similar sharp peak, albeit with somewhat higher T_m (67.5°C) is present in the DSC scan of the Vd1 complex with talin 482-636 (Fig 6B) indicating that Vd1 binds to talin 482-636 in a similar manner to the talin rod. The low T_m (53.9°C) and low unfolding enthalpy of the talin 482-636 4-helix bundle demonstrates that it is loosely folded, whilst the much higher T_m (60.2°C) and higher unfolding enthalpy of the talin 482-655 5-helix bundle (Fig 6C) shows that the additional helix stabilizes the bundle. These observations are in accord with the NMR data (52).

Incubation of the 482-636 polypeptide with Vd1 resulted in the formation of a 1:1 complex, and no free Vd1 remained (Fig 6B). This is consistent with ELISA data (Fig 2A and Fig 4A), and also gel filtration data which showed 1:1

high affinity binding between talin 482-636 and Vd1 (52). Interestingly, binding of the talin 482-655 polypeptide to Vd1 was also readily detected by DSC (Fig. 6C), whereas no binding was observed in ELISA, gel filtration or ITC experiments conducted at room temperature. During DSC experiments, the sample temperature is raised, and one can speculate that at the elevated temperatures, the talin 482-655 fold becomes destabilized permitting Vd1 binding. Interestingly, Vd1 seems to promote the destabilization of the talin 482-655 fold - there is a new peak with $T_m = 49.0^\circ\text{C}$ present in the DSC scan of the talin 482-655-Vd1 complex, but not in the scan of 482-655 alone (Fig 6C). This peak could represent melting of a fraction of unbound Vd1 or alternatively, melting of talin 482-655 destabilized by Vd1 binding. If the first scenario were correct, then increasing 482-655 concentration in the sample should decrease the intensity of this peak, since less unbound Vd1 will be present. In fact, raising the talin 482-655 concentration 1.5 fold (Fig 6C) caused a slight increase in the intensity of the 49.0°C peak. Thus this peak appears to represent melting of talin 482-655 destabilized by Vd1 binding. Together, these results demonstrate that the greater stability of the talin 482-655 5-helix bundle (domain 1) renders the VBS in helix 4 cryptic at room temperature. This conclusion was substantiated by analysing the ability of talin 482-655 to bind Vd1 at different temperatures using gel filtration (Fig 7). At 20°C, there was no evidence of binding although some complex formation could be detected at 37°C. Only when the temperature was increased to 45°C was stoichiometric binding of Vd1 to talin 482-655 observed.

Analysis of Vd1 binding to talin polypeptides 482-789 and 482-889 by DSC-To further investigate the relationship between helical bundle stability and vinculin binding, we next used DSC to analyse Vd1 binding to talin polypeptides containing domain1 and either part of, or the whole of domain 2 (residues 656-889), which contains four VBS's (Fig 1) one or more of which is active as indicated by ELISA, gel filtration and ITC experiments. The crystal structure of 482-789 reveals that the domain 1 5-helix bundle is followed by a 4-helix bundle which packs against domain 1 in a staggered manner (52). Interestingly, the melting temperature of talin 482-789 (70.4°C) (Fig 8A) was substantially higher than that of talin 482-655 (60.2°C) (Fig 6C)

indicating that domain 1 is further stabilised by the adjacent 4-helix bundle. Binding of the 482-789 polypeptide to Vd1 (Fig 8A) was greatly inhibited in DSC experiments in agreement with both the ELISA (Fig 4B) and gel filtration data (Fig 5B). We conclude that the 482-789 polypeptide adopts a very stable fold, and the additional VBS's in helices 6 and 9 are only partially active, even at elevated temperatures.

We have developed a model of talin 482-889 (53) from the crystal structure of 482-789 (52) and the NMR structure of talin 755-889 (53) which overlap by one helix. The model predicts that domain 1 is actually followed by a 7-helix bundle. When 482-889 was analysed by DSC (Fig 8C), the main peak was at 69.2°C with a shoulder at ~75°C. The fact that the T_m of the main peak (69.2°C) is 1.2°C less than that of the 482-789 polypeptide (70.4°C) suggests that in this case, the incorporation of an additional three helices has a destabilising effect on the overall fold adopted by the 7-helix bundle. Strong binding of Vd1 to 482-889 (Fig 8C) was detected by DSC in agreement with the data from ELISA (Fig 4B), gel filtration (Fig 5A) and ITC (K_d ~0.14 μ M; Table 1). The above results reinforce the idea that the activity of VBS's within the talin rod is in part determined by the stability of the helical bundles in which they are embedded.

A mutation that stabilises the talin 755-889 fold reduces Vd1 binding-The NMR structure of a talin 755-889 polypeptide reveals a 4-helix bundle (53) which contains 3 VBS's (Fig 1; helices 9, 11 and 12) all of which appear to be active as judged by NMR, native gels and gel filtration (53). Moreover, NMR shows that this talin polypeptide undergoes a major conformational change upon Vd1 binding, and the non-VBS helix 10 completely unfolds (52). However, DSC data shows that this 4-helix bundle has an unexpectedly high melting temperature (74.2°C), although DSC confirms that it does contain at least one active VBS (Fig 8B). Interestingly, it is not an effective competitor of GST-Vd1 binding to talin 482-636 in the ELISA assay (Fig 4B) presumably because the 755-889 fold is much more stable than the talin 482-636 polypeptide which has a T_m of 53.9°C.

To examine the relationship between fold stability and Vd1 binding directly, we introduced mutations into the talin 755-889 polypeptide that would be predicted to further stabilise the 755-889 four-helix bundle. This fold is characterised by two threonine pairs (Thr775/Thr809 and

Thr833/Thr867) that are accommodated within the hydrophobic core of the bundle (53). Mutation of these threonines to more hydrophobic residues would be expected to stabilise the fold and to reduce the availability of the VBS's contained therein. We therefore expressed a talin 755-889 mutant polypeptide in which these threonine pairs were replaced by isoleucine/valine pairs: Thr775Val/Thr809Ile/Thr833Ile/Thr867Val, referred to as the VIIV mutant. We confirmed that these mutations do not affect the capacity of GST-Vd1 to bind the VBS's contained within talin 755-889 using a SPOT-peptide assay (Supplementary Fig S1). The CD spectra of both the wild-type and VIIV mutant polypeptides were very similar and indicated, as expected, a predominantly helical fold (data not shown). Analysis of the change in the mean molar ellipticity at 222nm with increasing temperature showed a cooperative unfolding of the wild-type 755-889 polypeptide with a T_m of 72.6°C (Fig 9A), in good agreement with the DSC data. By contrast, the VIIV mutant was much more stable, and was less than 50% unfolded even at 95°C. The contrast in stabilities of the two proteins was further illustrated by experiments in 5.6M urea, where the T_m of the mutant was 78.4°C whereas the wild-type protein was completely unfolded even at 20°C under these conditions (data not shown). Gel filtration experiments showed that whereas wild-type 755-889 binds strongly to Vd1 (Fig 9B), the VIIV mutant binds much more weakly (Fig 9C); even with a three-fold excess of vinculin Vd1, less than half the mutant is in the form of the complex. The results clearly establish that the inherent stability of the individual amphipathic helical bundles making up the talin rod is likely to play a significant role in determining the activity of any VBS contained within the bundle.

Focal adhesion targeting of talin polypeptides containing VBS's-Talin polypeptides containing active VBS's would be expected to localise in vinculin-containing FAs when expressed in mammalian cells. To test this prediction, NIH3T3 cells were transfected with HA-tagged talin 482-636 or 482-655 in which VBS1 is constitutively active or cryptic respectively. As predicted, the 482-636 polypeptide localised to FAs whereas the 482-655 did not (Fig 10). In contrast, a talin 482-636 polypeptide containing a double mutation in the VBS which abolishes Vd1 binding in vitro (52), failed to localise to FAs. These results support the conclusion that localisation of these

talin polypeptides to FAs reflects the activity of the VBS. We then transfected cells with HA-tagged talin 482-789 and 482-889 constructs. Interestingly, only talin 482-889 localised to FAs. Collectively, the foregoing results indicate that although there are 3 VBS's within residues 482-789, they are not fully available for vinculin binding, whereas extension of the polypeptide by an additional 3 helices (two of which contains VBS's) results in a polypeptide (482-889) that can support vinculin binding in vitro and in vivo.

DISCUSSION

The VBS's in the talin rod are defined by hydrophobic residues on one face of a series of amphipathic helices. However, crystallographic (52) and NMR (53) structures of domains of the talin rod show that the key residues are normally buried within the hydrophobic cores of α -helical bundles. Indeed, mutagenesis shows that the VBS residues contribute to interhelical contacts, and the stability of the bundle (52). In agreement with these observations, the competitive ELISA and ITC data shown here clearly indicate that most of the VBS's in either gizzard talin or recombinant talin are in a low affinity state, although the fact that Vd1 binding could be detected in pull down and ITC assays demonstrates that one or more VBS's in talin are available for binding. The finding that Vd1 exposes a cryptic trypsin cleavage site towards the N-terminal region of the talin rod (between residues 898/899) strongly suggests that there is at least one active VBS in this vicinity. Since the remainder of the talin rod remains resistant to proteolysis in the presence of Vd1, we surmise that the VBS's contained therein must be in a low affinity state.

It is notable that the N-terminal region of the talin rod contains 5 out of the ~11 VBS's in talin (Fig 1) (49). Structures of this region show that it is comprised of two domains (52,53). Domain 1 (residues 482-655) is a five helix bundle containing one VBS (helix 4), but this is cryptic at room temperature as shown by competitive ELISA, gel filtration and ITC data. Domain 2 appears to be a seven helix bundle (residues 656-889), and contains four VBS's (helices 6, 9, 11 and 12). One or more of these sites is active because talin 482-889 binds strongly to Vd1 in ELISA, DSC and ITC experiments. Moreover, gel filtration experiments indicate that three of the VBS's in the talin 482-889 polypeptide are active.

It is interesting that the ~50 kDa N-terminal tryptic fragment (residues 482-898) liberated from the talin rod in the presence of Vd1 is almost completely degraded, suggesting that the entire region undergoes a marked conformational rearrangement upon Vd1 binding. This is reminiscent of the effects of Vd1 on the conformation of recombinant talin polypeptides containing active VBS's as seen by both NMR and enhanced sensitivity to proteolysis. Indeed Vd1 induces the complete unfolding of one of the helices in the talin 755-889 four helix bundle (53). The data suggest that vinculin binding to one or more VBS's within residues 655-889 induces a conformational change that is propagated throughout the whole region, and this may lead to activation of previously cryptic or low affinity sites.

Why one or more of the VBS's in domain 2 of the talin rod are able to bind vinculin whilst other VBS's in the talin rod are in a low affinity state requires further investigation. The data reported here suggest that one important factor is the inherent stability of the helical bundle in which a VBS is embedded. This is readily illustrated by reference to the data on domain 1 that contains a single cryptic VBS (helix 4). DSC shows that the 5-helix bundle melts at 60.2°C. Removal of helix 5 destabilises the bundle as indicated by the lower melting temperature (53.0°C) and by NMR (53), and the resulting four helix bundle binds Vd1 with high affinity. Interestingly, although the five helix bundle is unable to bind Vd1 at room temperature, it will bind Vd1 in both DSC and gel filtration experiments conducted at higher temperatures, presumably because the five-helix bundle is less stable under these conditions. Similarly, mutations to the hydrophobic core of the bundle that would be predicted to destabilise the bundle also activate Vd1 binding (52). In the slightly larger talin 482-789 polypeptide, the five helix bundle is followed by a four helix bundle, and this polypeptide contains three VBS's (helices 4, 6 and 9). Although it does bind Vd1 in both gel filtration and competitive ELISA, the affinity is much lower than for the 482-636 four helix bundle. Interestingly, the 482-789 polypeptide melts at a higher temperature (70.4°C) than the talin 482-655 polypeptide (60.2°C), indicating that domain 1 is stabilised by the adjacent four helix bundle, and even in DSC, binding to Vd1 is greatly inhibited. The picture is quite different with the talin 482-889 polypeptide that contains an additional three

helices two of which (helices 11 and 12) are VBS's. This polypeptide binds Vd1 with high affinity and melts at a slightly lower temperature (69.2°C) than the 482-789 polypeptide (70.4°C) indicating that inclusion of the additional three helices has a slight destabilising effect on the domain 2 fold. Moreover, the 482-889 polypeptide is cleaved by trypsin at residue 790 removing the last three helices (data not shown), suggesting that these are somewhat less stable and/or less tightly packed against the other helices. Therefore, we tentatively conclude that it is this region in intact talin that contains the active VBS's since Vd1 induces trypsin cleavage nearby (i.e. between residues 898/899).

A direct test of the relationship between fold stability and Vd1 binding was carried out by constructing a mutant of the 755-889 four-helix bundle Thr775Val/Thr809Ile/Thr833Ile/Thr867Val predicted to have a more stable fold. In line with prediction, this mutant was substantially more stable to thermal and urea denaturation, and was also markedly less effective at binding Vd1. Taken together, our results clearly establish that the inherent stability of the amphipathic helical bundles that make up the talin rod is an important determinant of vinculin binding. This is borne out by studies on the localisation of HA-tagged talin polypeptides expressed in NIH3T3 cells. Thus, those which bind Vd1 with high affinity in vitro (482-636, 482-889) target to FAs, whereas those that do not bind

(482-655), or bind with low affinity (482-789) fail to do so. A simple general correlation between overall thermal stability and Vd1 binding would only be expected if the talin bundle unfolded before interaction with Vd1; it is perhaps more likely that an initial interaction with Vd1 is required to initiate the structural changes in the talin bundle to expose the VBS, so that the stability of the fold will not be the only factor.

Talin is ubiquitously expressed, and is found in structures ranging from the myotendinous junction (58) and costameres in skeletal muscle (59), the intercalated discs in cardiac muscle (59), dense plaques in smooth muscle (60), the neuromuscular junction (61), the immunological synapse (62), neuronal growth cones, the synapse (63), phagocytic cups (64) and the mid-body in cytokinesis (65). Talin typically colocalises with vinculin, and it may be significant that in most of these structures, the integrin/talin complex is subject to force induced by actomyosin contraction. This raises the possibility that force induced unfolding of the helical bundles in talin may be a significant factor in the exposing VBS's in the talin rod. Since vinculin is also an F-actin binding protein (66,67), it may be recruited to strengthen the link between talin and F-actin (45). Interestingly, in the immunological synapse, the integrin LFA-1/talin complex in T-cells does not colocalise with vinculin (62). Perhaps the junction between T-cells and antigen presenting cells is not subject to actomyosin contractile forces.

REFERENCES

1. Calderwood, D. A., Huttenlocher, A., Kiosses, W.B., Rose, D.M., Woodside, D.G., Schwartz, M.A., and Ginsberg, M.H. (2001) *Nature Cell Biol.* **3**, 1060-1068
2. Otey, C. A., Vasquez, G.B., Burrige, K., and Erickson, B.W. (1993) *J. Biol. Chem.* **268**, 21193-21197
3. Calderwood, D. A., Fujioka, Y., de Pereda, J. M., Garcia-Alvarez, B., Nakamoto, T., Margolis, B., McGlade, C. J., Liddington, R. C., and Ginsberg, M. H. (2003) *Proc Natl Acad Sci U S A* **100**, 2272-2277
4. Torgler, C. N., Narasimha, M., Knox, A. L., Zervas, C. G., Vernon, M. C., and Brown, N. H. (2004) *Dev Cell* **6**, 357-369
5. Zervas, C. G., Gregory, S. L., and Brown, N. H. (2001) *J Cell Biol* **152**, 1007-1018
6. Burrige, K., and Connell, L. (1983) *J Cell Biol* **97**, 359-367
7. Horwitz, A., Duggan, K., Buck, C., Beckerle, M. C., and Burrige, K. (1986) *Nature* **320**, 531-533
8. Bolton, S. J., S.T. Barry, H. Mosley, B. Patel, B.M. Jockusch, J.M. Wilkinson, and D.R. Critchley. (1997) *Cell Motil. Cytoskeleton* **36**, 363-376
9. Nuckolls, G. H., Romer, L.H., Burrige, K. (1992) *J. Cell Sci.* **102**, 753-762
10. Sydor, A. M., A.L. Su, F-S. Wang, A. Xu, and D.G. Jay. (1996) *J. Cell Biol.* **134**, 1197-1207
11. Albiges-Rizo, C., Frachet, P., and Block, M.R. (1995) *J. Cell Sci.* **108**, 3317-3329.

12. Jiang, G., Giannone, G., Critchley, D. R., Fukumoto, E., and Sheetz, M. P. (2003) *Nature* **424**, 334-337
13. Giannone, G., Jiang, G., Sutton, D. H., Critchley, D. R., and Sheetz, M. P. (2003) *J Cell Biol* **163**, 409-419
14. Priddle, H., Hemmings, L., Monkley, S., Woods, A., Patel, B., Sutton, D., Dunn, G.A., Zicha, D., and Critchley, D.R. (1998) *J. Cell Biol.* **142**, 1121-1133
15. Monkley, S. J., Zho, X-H., Kinston, S.J., Giblett, S.M., Hemmings, L., Priddle, H., Brown, J.E., Pritchard, C.A., Critchley, D.R. and Fassler, R. (2000) *Dev. Dynamics* **219**, 560-574
16. Brown, N. H., Gregory, S.L., Rickoll, W.L., Fessler, L.I., Prout, M., White, R.A. and Fristrom, J.W. (2002) *Dev. Cell* **3**, 569-579
17. Cram, E. J., Clark, S. G., and Schwarzbauer, J. E. (2003) *J Cell Sci* **116**, 3871-3878
18. Monkley, S. J., Pritchard, C.A. and Critchley, D.R. (2001) *Biochem Biophys Res Commun.* **286**, 880-885
19. Winkler, J., H. Lunsdorf, and B.M. Jockusch. (1997) *Eur. J. Biochem.* **243**, 430-436
20. Isenberg, G., and Goldmann, W. H. (1998) *FEBS Letts.* **426**, 165-170
21. Calderwood, D. A., Zent, R., Grant, R., Rees, D. J. G., Hynes, R. O., and Ginsburg, M. H. (1999) *J. Biol. Chem.* **274**, 28071-28704
22. Garcia-Alvarez, B., de Pereda, J. M., Calderwood, D. A., Ulmer, T. S., Critchley, D., Campbell, I. D., Ginsberg, M. H., and Liddington, R. C. (2003) *Mol. Cell* **11**, 49-58
23. Borowsky, M. L., and Hynes, R. O. (1998) *J. Cell Biol.* **143**, 429-442
24. Lee, H. S., Bellin, R. M., Walker, D. L., Patel, B., Powers, P., Liu, H., Garcia-Alvarez, B., de Pereda, J. M., Liddington, R. C., Volkman, N., Hanein, D., Critchley, D. R., and Robson, R. M. (2004) *J Mol Biol* **343**, 771-784
25. Ling, K., Doughman, R. L., Firestone, A. J., Bunce, M. W., and R.A., A. (2002) *Nature* **420**, 89-93
26. Ling, K., Doughman, R. L., Iyer, V. V., Firestone, A. J., Bairstow, S. F., Mosher, D. F., Schaller, M. D., and Anderson, R. A. (2003) *J Cell Biol* **163**, 1339-1349
27. Di Paolo, G., Pellegrini, L., Letinic, K., Cestra, G., Zoncu, R., Voronov, S., Chang, S., Guo, J., Wenk, M.R. and De Camilli, P. (2002) *Nature* **420**, 85-89
28. Barsukov, I. L., Prescott, A., Bate, N., Patel, B., Floyd, D. N., Bhanji, N., Bagshaw, C. R., Letinic, K., Di Paolo, G., De Camilli, P., Roberts, G. C., and Critchley, D. R. (2003) *J Biol Chem* **278**, 31202-31209
29. de Pereda, J. M., Wegener, K. L., Santelli, E., Bate, N., Ginsberg, M. H., Critchley, D. R., Campbell, I. D., and Liddington, R. C. (2005) *J Biol Chem* **280**, 8381-8386
30. Muguruma, M., Nishimuta, S., Tomisaka, Y., Ito, T. and Matsumara, S. (1995) *J. Biochem.* **117**, 1036-1042
31. Hemmings, L., D.J.G. Rees, V. Ohanian, S.J. Bolton, A.P. Gilmore, N. Patel, H. Priddle, J.E. Trevithick, R.O. Hynes and D.R. Critchley. (1996) *J. Cell Sci.* **109**, 2715-2726
32. Tremuth, L., Kreis, S., Melchior, C., Hoebeke, J., Ronde, P., Plancon, S., Takeda, K., and Kieffer, N. (2004) *J Biol Chem* **279**, 22258-22266
33. Bass, M. D., Smith, B.J., Prigent, S.A. and Critchley, D.R. (1999) *Biochem. J.* **341**, 257-263
34. Jockusch, B. M., Rudiger, M. (1996) *Trends Cell Biol.* **6**, 311-315
35. Martel, V., Racaud-Sultan, C., Dupe, S., Marie, C., Paulhe, F., Galmiche, A., Block, M. R., and Albiges-Rizo, C. (2001) *J. Biol. Chem.* **276**, 21217-21227.
36. Tadokoro, S., Shattil, S. J., Eto, K., Tai, V., Liddington, R. C., de Pereda, J. M., Ginsberg, M. H., and Calderwood, D. A. (2003) *Science* **302**, 103-106
37. Kim, M., Carman, C. V., and Springer, T. A. (2003) *Science* **301**, 1720-1725
38. Critchley, D. R. (2004) *Biochem Soc Trans* **32**, 831-836
39. Rodriguez Fernandez, J. L., Geiger, B., Salomon, D., Benzeev, A. (1993) *J. Cell Biol.* **122**, 1285-1294
40. Rodriguez Fernanedez, J. L., Geiger, B., Salomon, D., and Ben Ze'ev, A.,. (1992) *Cell Motil. Cytoskeleton* **22**, 127-134

41. Coll, J.-L., Ben Ze'ev, A., Ezzell, R. M., Rodriguez-Fernandez, J. L., Baribault, H., Oshima, R. G., and Adamson, E. D. (1995) *Proc. Natl. Acad. Sci. USA* **92**, 9161-9165.
42. Volberg, T., Geiger, B., Kam, Z., Pankov, R., Simcha, I., Sabanay, H., Coll, J.-L., Adamson, E., Ben-Ze'ev, A. (1995) *J. Cell Sci.* **108**, 2253-2260
43. Xu, W., Coll, J.-L. and Adamson, E.D. (1998) *J. Cell Sci.* **111**, 1535-1544
44. Xu, W., Baribault, H., and Adamson, E.D. (1998) *Development* **125**, 327-337
45. Galbraith, C. G., Yamada, K. M., and Sheetz, M. P. (2002) *J Cell Biol* **159**, 695-705
46. Gilmore, A. P., Wood, C., Ohanian, V., Jackson, P., Patel, B., Rees, D. J. G., Hynes, R. O., and Critchley, D. R. (1993) *J. Cell Biol.* **122**, 337-347
47. Bass, M. D., Patel, B., Barsukov, I.G., Fillingham, I.J., Mason, R., Smith, B.J., Bagshaw, C.R., and Critchley, D.R. (2002) *Biochem. J.* **362**, 761-768
48. McLachlan, A. D., Stewart, M., Hynes, R.O., Rees, D.J.G. (1994) *J. Mol. Biol.* **235**, 1278-1290
49. Gingras, A. R., Ziegler, W. H., Frank, R., Barsukov, I. L., Roberts, G. C., Critchley, D. R., and Emsley, J. (2005) *J Biol Chem* **280**, 37217-37224
50. Izard, T., Evans, G., Borgon, R. A., Rush, C. L., Bricogne, G., and Bois, P. R. (2004) *Nature* **427**, 171-175
51. Izard, T., and Vonrhein, C. (2004) *J Biol Chem* **279**, 27667-27678
52. Papagrigoriou, E., Gingras, A. R., Barsukov, I. L., Bate, N., Fillingham, I. J., Patel, B., Frank, R., Ziegler, W. H., Roberts, G. C., Critchley, D. R., and Emsley, J. (2004) *Embo J* **23**, 2942-2951
53. Fillingham, I., Gingras, A. R., Papagrigoriou, E., Patel, B., Emsley, J., Critchley, D. R., Roberts, G. C., and Barsukov, I. L. (2005) *Structure (Camb)* **13**, 65-74
54. Bakolitsa, C., Cohen, D. M., Bankston, L. A., Bobkov, A. A., Cadwell, G. W., Jennings, L., Critchley, D. R., Craig, S. W., and Liddington, R. C. (2004) *Nature* **430**, 583-586
55. Rees, D. J. G., Ades, S. E., Singer, S. J. and Hynes, R. O. (1990) *Nature* **347**, 685-689
56. Johnson, R. P., and Craig, S. W. (1994) *J. Biol. Chem.* **269**, 12611-12619
57. Yan, B., Calderwood, D. A., Yaspan, B., and Ginsberg, M. H. (2001) *J Biol Chem* **276**, 28164-28170
58. Tidball, J. G., Ohalloran, T., and Burrige, K. (1986) *J.Cell Biol.* **103**, 1465-1472
59. Belkin, A. M., Zhidkova, N. I., and Koteliansky, V. E. (1986) *FEBS Lett.* **200**, 32-36
60. Volberg, T., Sabanay, H., and Geiger, B. (1986) *J. Muscle Res. Cell Motil.* **7**, 375-376
61. Sealock, R., Paschal, B., Beckerle, M., and Burrige, K. (1986) *Experimental Cell Research* **163**, 143-150
62. Monks, C. R. F., Freiberg, B. A., Kupfer, H., Sciaky, N., and Kupfer, A. (1998) *Nature* **395**, 82-86
63. Morgan, J. R., Di Paolo, G., Werner, H., Shchedrina, V. A., Pypaert, M., Pieribone, V. A., and De Camilli, P. (2004) *J Cell Biol* **167**, 43-50
64. Greenberg, S., Burrige, K., and Silverstein, S. C. (1990) *J. Exp. Med.* **172**, 1853-1856
65. Bellissent-Waydelich, A., Vanier, M-T., Albiges-Rizo, C., and Simon-Assmann, P. (1999) *J. Histochem. Cytochem.* **47**, 1357-1367
66. Menkel, A. R., Kroemker, M., Bubeck, P., Ronsiek, M., Nikolai, G., Jockusch, B.M. (1994) *J.Cell Biol.* **126:5**, 1287-1298
67. Huttelmaier, S., Bubeck, P., Rudiger, M., and Jockusch, B. M. (1997) *Eur. J. Biochem.* **247**, 1136-1142
68. Schmidt, J. M., Zhang, J., Lee, H.-S., Stromer, M. H., and Robson, R. M. (1999) *Archives Biochem. Biophys.* **366**, 139-150

FOOTNOTES

The work at the University of Leicester was supported by grants from BBSRC and the Wellcome Trust, and that at the Burnham Institute was supported by grant 5 U54 GM64346 from NIH to the Cell Migration Consortium. The authors are grateful to Dr Sharad Mistry in the Protein and Nucleic Acid Laboratory, University of Leicester for N-terminal sequencing of talin polypeptides. We thank Dr. Laurie Bankston and Greg Cadwell for their help in preparation of proteins for ITC experiments.

FIGURE LEGENDS

Fig 1. Schematic diagram of talin and the talin polypeptides used in this study. Talin contains an N-terminal FERM domain linked to the talin rod which is made up of ~62 amphipathic helices (grey ovals) certain of which have vinculin binding activity (dark grey). The relative positions of the other ligand binding sites in talin are also indicated. The various talin polypeptides used in this study are shown at the bottom of the figure. Helices are depicted as cylinders – those in dark grey contain vinculin binding sites. These are numbered according to their position within the full-length talin rod.

Fig 2. The vinculin-binding sites (VBS's) in talin are in a low affinity state. [A] The ability of GST-vinculin head residues 1-258 (Vd1) to bind talin was assessed using a competition ELISA-based assay at 490nm (52). Microtitre wells were coated with a talin polypeptide spanning residues 482-636 which contains a single VBS that is constitutively active. Binding of GST-Vd1 was determined by ELISA in the presence of increasing concentrations (nM) of talin or talin polypeptides. In one case, the talin was preincubated with PIP2 (100x molar excess). [B] Binding of GST-Vd1 to talin determined using a pull down assay. Bound talin was resolved by SDS-PAGE and detected by Western blotting with mouse monoclonal TD77 (epitope 2494-2541). Talin purified from turkey gizzard (68) was (a) stained with Coomassie blue or (b) detected by Western blotting with TD77. (c) Binding of talin to GST alone. (d) Binding of talin to GST-Vd1.

Fig 3. Vinculin binding to talin exposes a cryptic trypsin cleavage site in the talin rod. Purified turkey gizzard talin was incubated with trypsin (lanes 2, 4) in the absence (lane 2) or presence (lane 4) of vinculin Vd1. Samples were analysed by SDS-PAGE and talin was detected by staining with [A] Coomassie blue, [B] monoclonal antibody 8d4 (epitope residues 482-655), [C] monoclonal antibody Td77 (epitope residues 2494-2541). The N-terminal sequence of the talin polypeptide (arrow) in panel [A] starts at residue 899. Right - molecular mass markers (kDa). Note the Vd1 (~28 kDa) has run off the bottom of the gel.

Fig 4. Talin residues 482-889 contain one or more active VBS's. Binding of GST-vinculin Vd1 to microtitre wells coated with talin polypeptide 482-636 was determined by ELISA (490nm) (52) in the presence of increasing concentrations (nM) of talin polypeptides. [A] 482-636, 482-655. [B] 755-889, 482-789 and 482-889.

Fig 5. Analysis of vinculin Vd1 binding to talin 482-889 and 482-789 by gel filtration. Superdex-75 (10/30) gel filtration chromatography of [A] talin 482-889 (0.05 mM) in the presence or absence of the vinculin Vd1 domain. Fractions (0.5 ml) were collected and analysed using 15% SDS-PAGE. At a 1:1 molar ratio of talin 482-889 / Vd1 (solid line), all the Vd1 is in complex with the talin polypeptide indicative of a high affinity interaction (the complex elutes at approximately the same position as free talin polypeptide). At a 1:3 molar ratio (dotted line), the complex elutes slightly ahead of the free talin polypeptide, and some free Vd1 is detected both by gel filtration (arrow) and SDS-PAGE. [B] Talin 482-789 [0.05mM] alone (dotted line) and Vd1 alone (not shown) elute at about the same position. At a 1:1 molar ratio of talin 482-789 / Vd1 (dashed line), a small amount of the Vd1 is in complex with the talin polypeptide (complex elutes at about 9 ml). At a molar ratio of 1:7 (solid line), an extra shift is observed in the elution of the complex (about 8 ml) but much of the Vd1 remains unbound.

Fig 6. Analysis of vinculin Vd1 binding to the talin rod, and to talin 482-636 and 482-655 talin polypeptides by Differential Scanning Calorimetry (DSC) and gel filtration. DSC scans are shown for [A] Vd1 (black), talin rod (Tr - green), and talin rod plus Vd1 at 1/1 molar ratio (red); dotted line indicates the difference profile (complex minus talin rod alone). [B] Vd1 (black), talin 482-636 (green), and talin 482-636 plus Vd1 at 1/1 molar ratio (red); [C] Vd1 (black), talin 482-655 (green), talin 482-655 plus Vd1 at 1/1 (red) and 3/2 (blue) molar ratios.

Fig 7. Gel filtration analysis of Vd1 binding to talin 482-655 at different temperatures. The talin 482-655 polypeptide was incubated with vinculin Vd1 for 30 minutes at either; [A] room temperature, [B] 37°C or 45°C. The mixture was then loaded onto a Superdex-75 (10/30) gel filtration column at room temperature. There was no complex formation between the two proteins at room temperature. Although complex could be detected at 37°C, most of the talin and vinculin polypeptides remained in the free form. However, at 45°C, >90% of the protein is in complex.

Fig 8. Analysis of vinculin Vd1 binding to talin 482-789, 755-889 and 482-889 polypeptides by Differential Scanning Calorimetry. DSC scans are shown for [A] Vd1 (black), talin 482-789 (green), and talin 482-789 plus Vd1 at 1/1 molar ratio (red); [B] Vd1 (black), talin 755-889 (green), and talin 755-889 plus Vd1 at 1/1 molar ratio (red); [C] Vd1 (black), talin 482-889 (green), talin 482-889 plus Vd1 at 1/1 molar ratio (red). Dotted line in [C] indicates the difference profile (complex minus 482-889 alone).

Fig 9. The talin 755-889 VIIV mutant is more stable and shows reduced vinculin Vd1 binding. [A] Denaturation profiles of wild-type talin 755-889 (black circles) and the quadruple VIIV mutant (white triangles) measured by monitoring the change in mean residue molar ellipticity at 222 nm ($[\theta]_{222}$) with increasing temperature. [B,C] Binding of wild-type talin 755-889 [B] and the quadruple VIIV mutant [C] to vinculin Vd1 determined by Superdex-75 (10/30) gel filtration chromatography. [B] At a 1:1 molar ratio of talin 755-889 / Vd1 (dot trace), all the Vd1 is in complex with the talin polypeptide. At a 1:3 molar ratio (line-dot trace), free Vd1 is detected, but all the talin 755-889 is in complex. [C] In contrast, at a 1:1 molar ratio of the talin 755-789 VIIV mutant / Vd1 (dot trace), most of the talin mutant and Vd1 are in their free form although some of the Vd1 is in complex with the talin polypeptide (complex elutes at ~ 8 ml). At a molar ratio of 1:3 (line-dot trace), there is an increase in complex assembly, but still, most of the two proteins remain in the free form.

Fig 10. Talin polypeptides which bind vinculin Vd1 target to focal adhesions. NIH 3T3 cells were grown on glass coverslips and transiently transfected with cDNAs encoding the HA-tagged talin polypeptides indicated. After 16 hr, the cells were stained with anti-HA followed by incubation with FITC-conjugated secondary antibody. F-actin was visualized with phalloidin-Texas Red (Molecular Probes). Actin staining and merged images are shown just for the HA-tagged talin polypeptides that localized in FAs. Results are representative of 3-6 separate experiments. Scale bar 10 μ m. The expression of the various talin polypeptides was confirmed by Western blotting using an anti-HA antibody. Talin polypeptides (482-655, 482-789 and 482-636M (52)) that have a low affinity for vinculin remain diffusely distributed within the cell, whereas those that bind vinculin with high affinity (482-636 and 482-889) localize to the end of actin filaments in FAs.

Supplementary Fig S1. Analysis of GST-Vd1 binding to talin rod helices 9, 10,11, and 12 using a SPOT-peptide assay. Talin rod helices 9, 10, 11, and 12 were spot synthesized, both as wild-type peptides and with the same point mutation used in the talin 755-889 VIIV mutant (Thr775Val/Thr809Ile/Thr833Ile/Thr867Val). The effects of each substitution on GST-Vd1 binding was then determined using a polyclonal GST antibody and alkaline phosphatase (AP)-coupled anti-rabbit Ig as described previously (49). The results of the binding assay are shown on the left of the corresponding peptide sequence. For each peptide, the substituted positions are highlighted in red. The analysis shows that the mutations caused no reduction in GST-Vd1 binding to talin VBS helices 9,11, and 12. Note that helix 10 does not bind GST-Vd1.

Table 1. Affinity of vinculin head (Vd1) for talin and talin fragments determined by ITC.

	K_d (μ M)
Talin	8.9 ± 3.4
Talin + PIP2	4.7 ± 1.6
Talin rod	2.4 ± 1.2
482-636	0.3 ± 0.1
482-655	No binding
482-889	0.14 ± 0.01

Figure 1

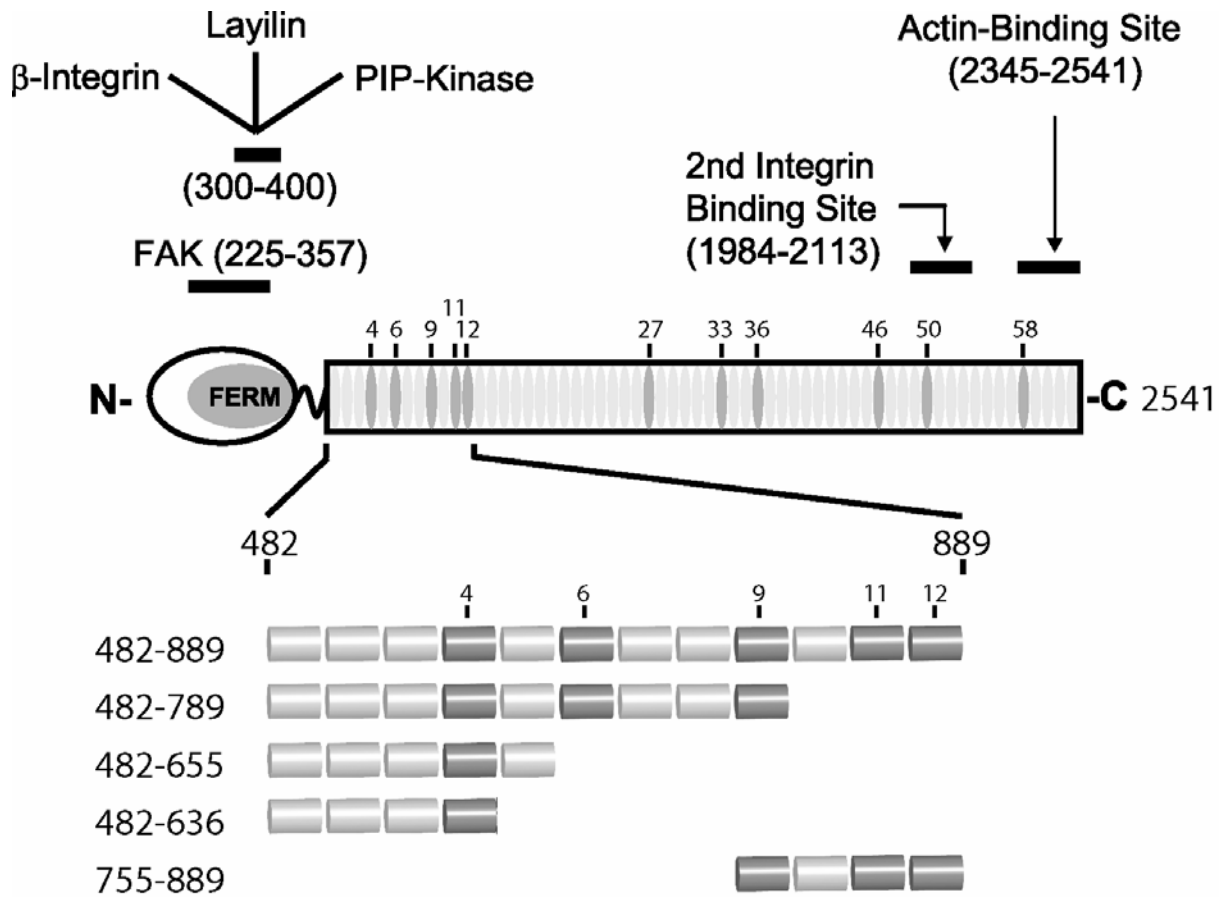


Figure 2

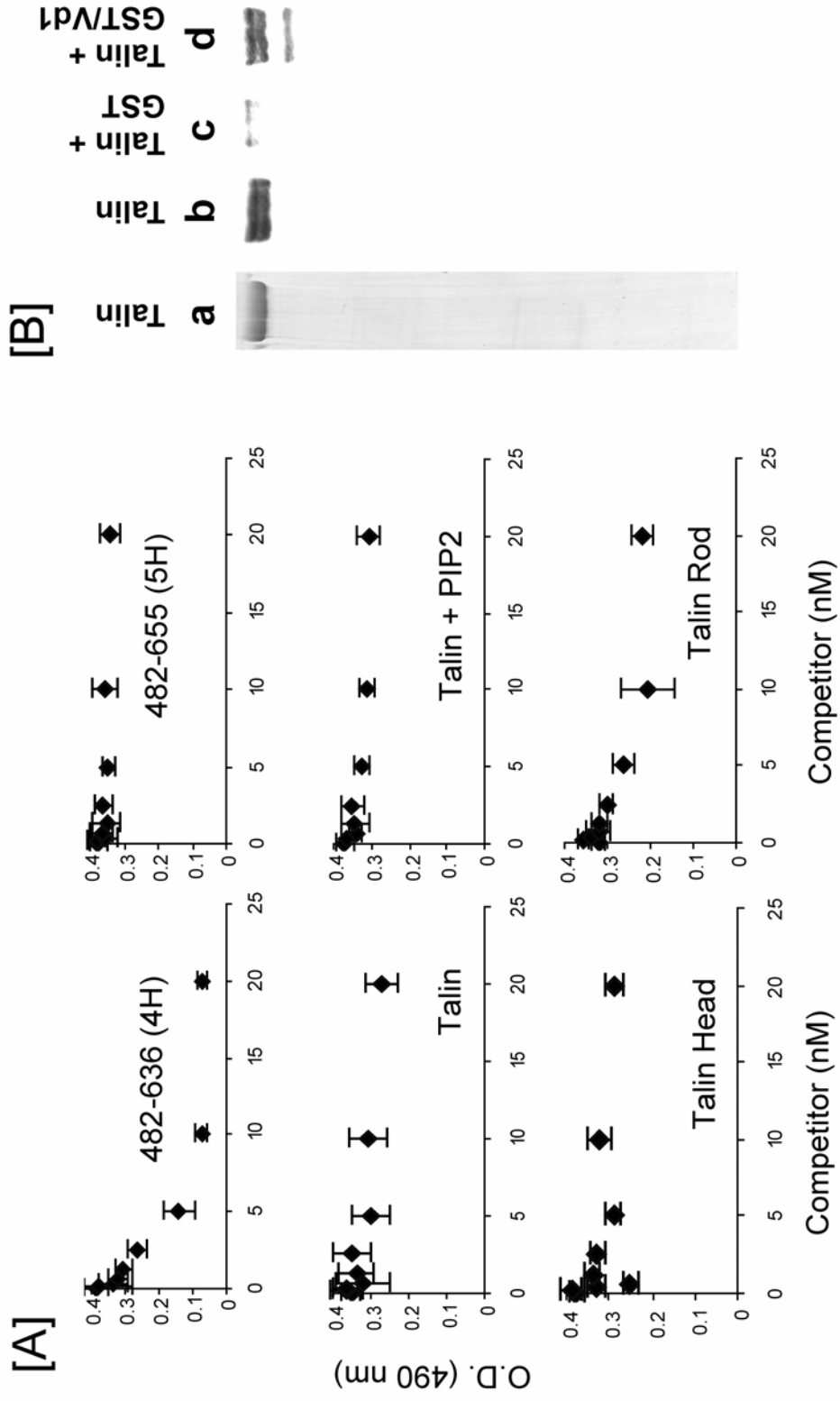


Figure 3

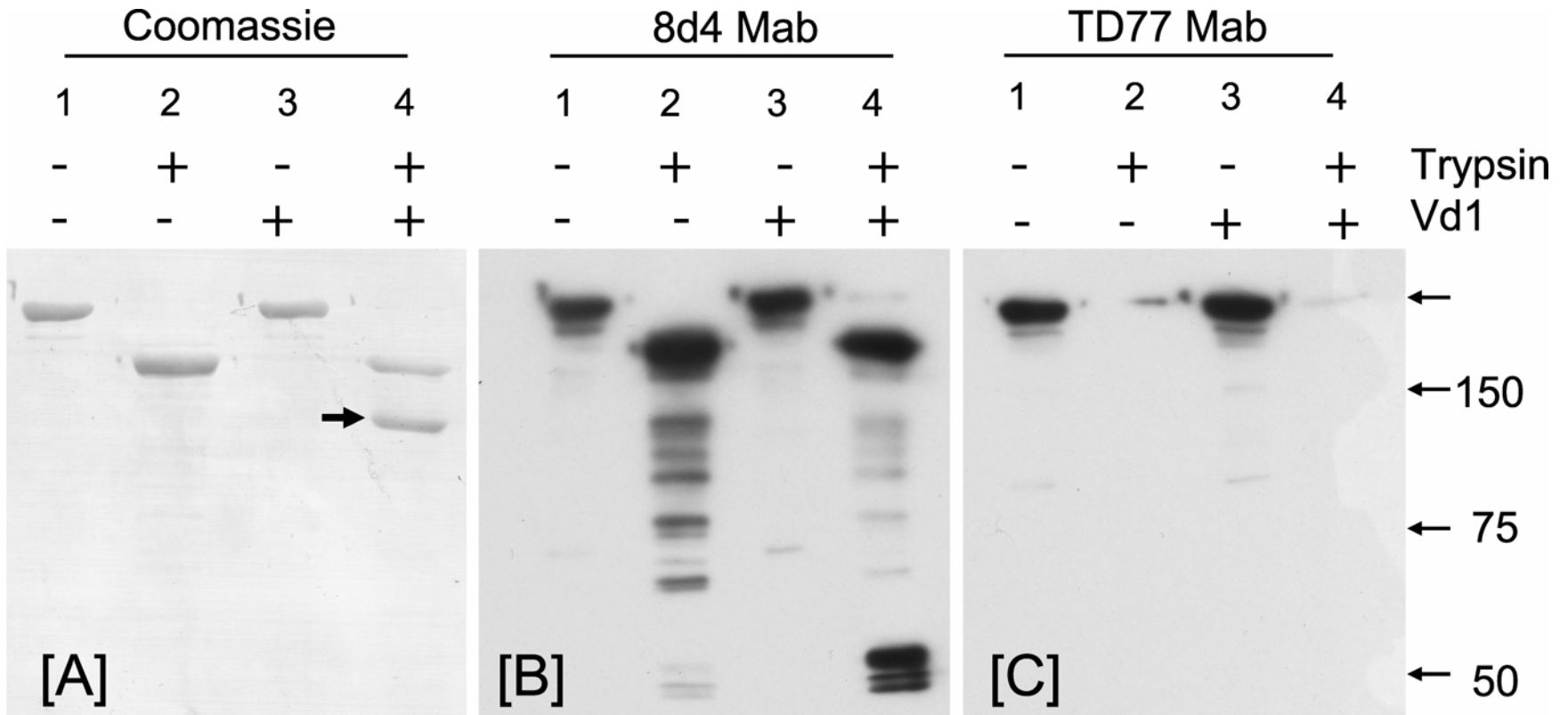


Figure 4

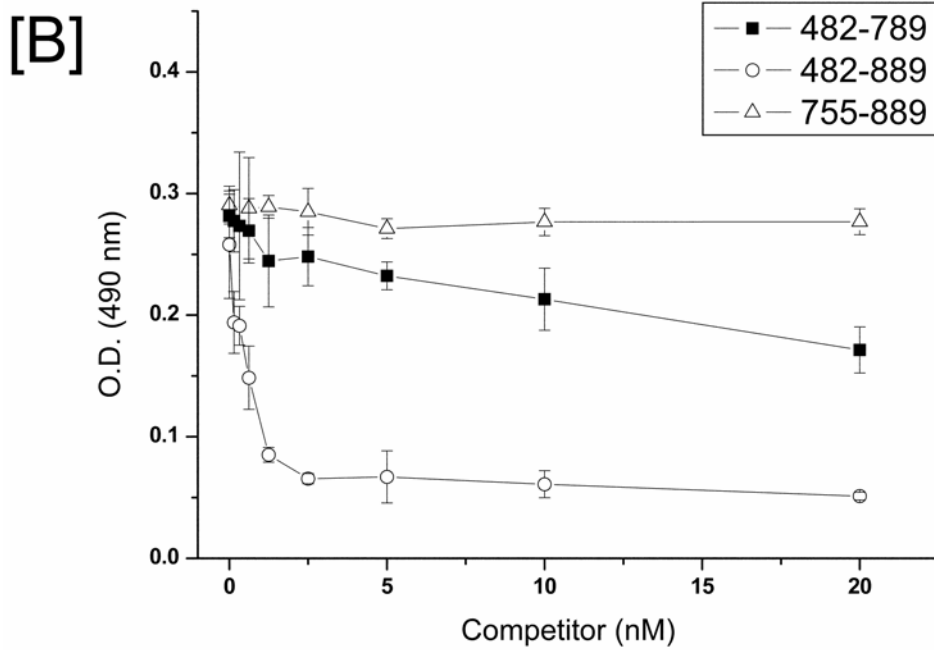
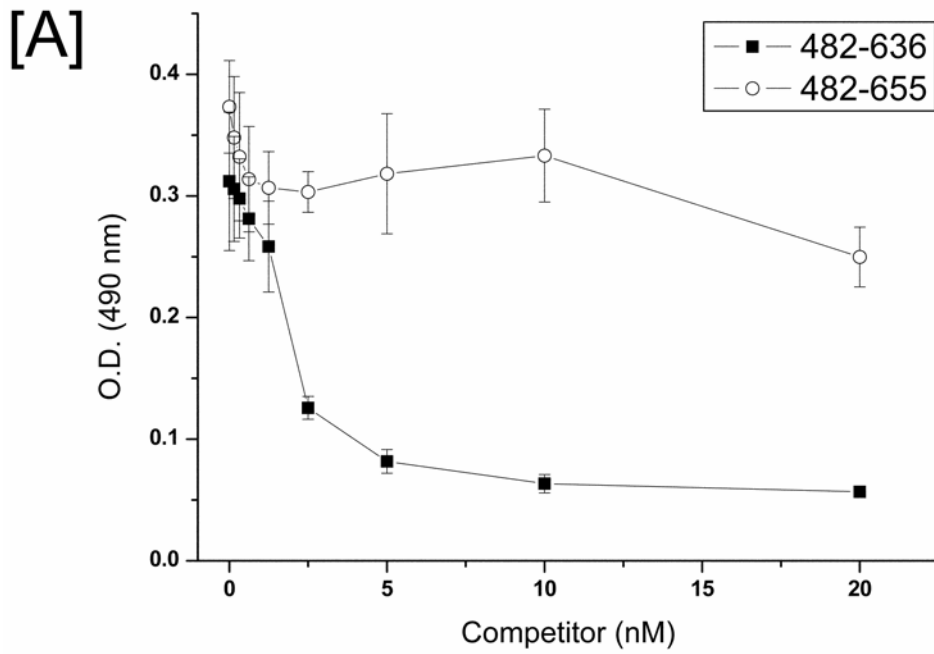


Figure 5

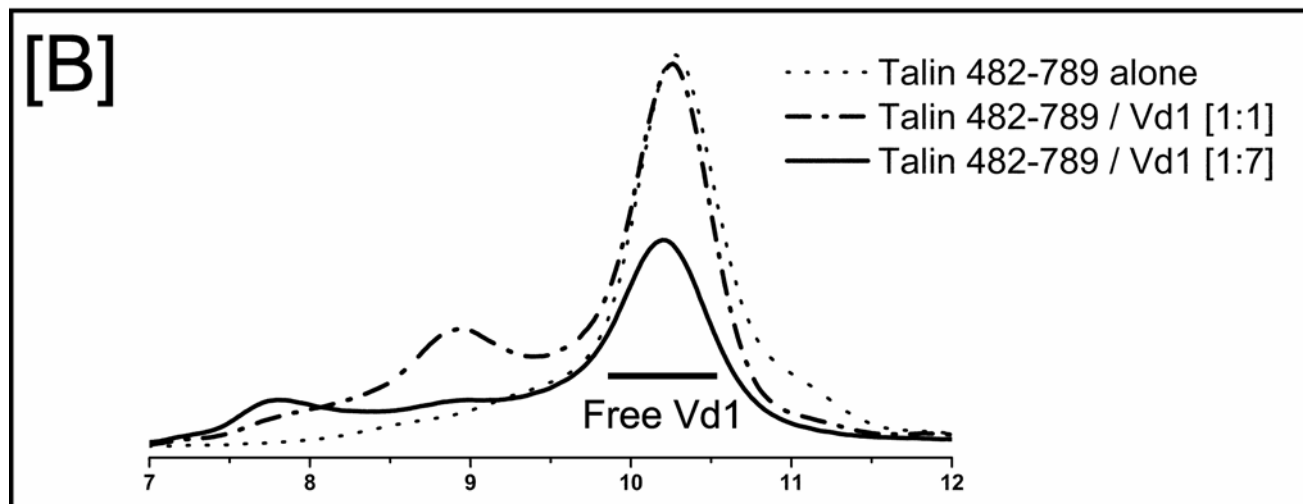
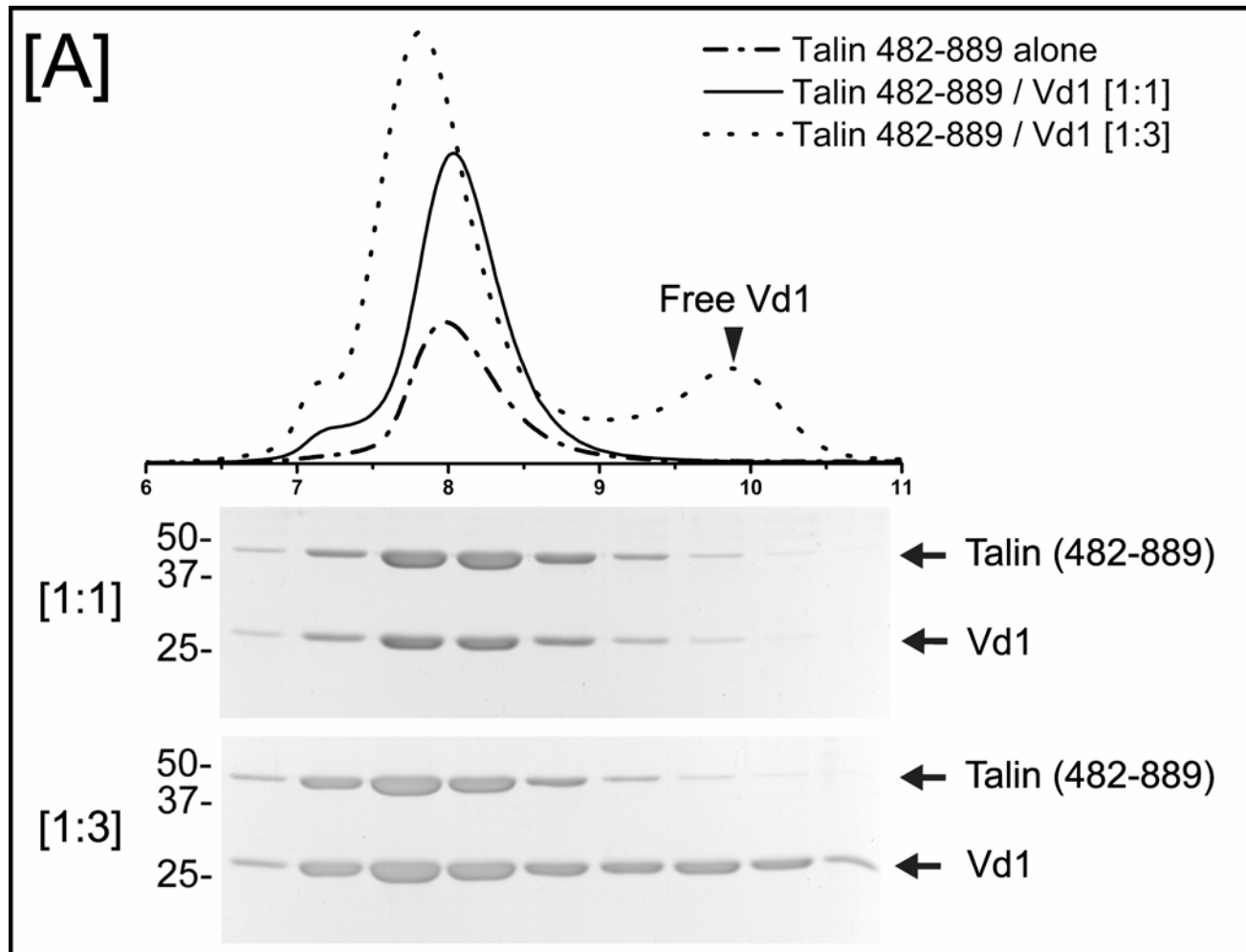


Figure 6

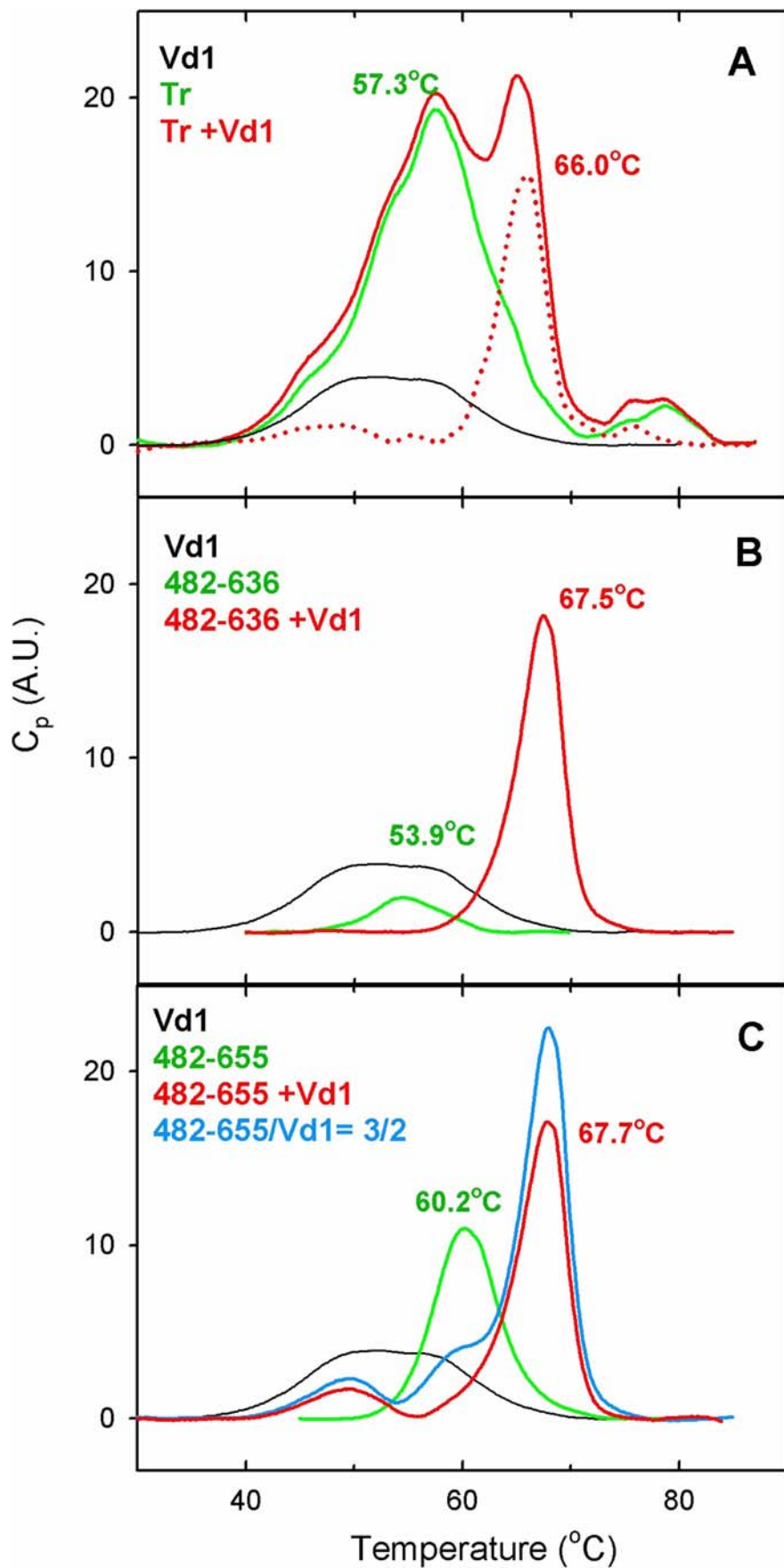
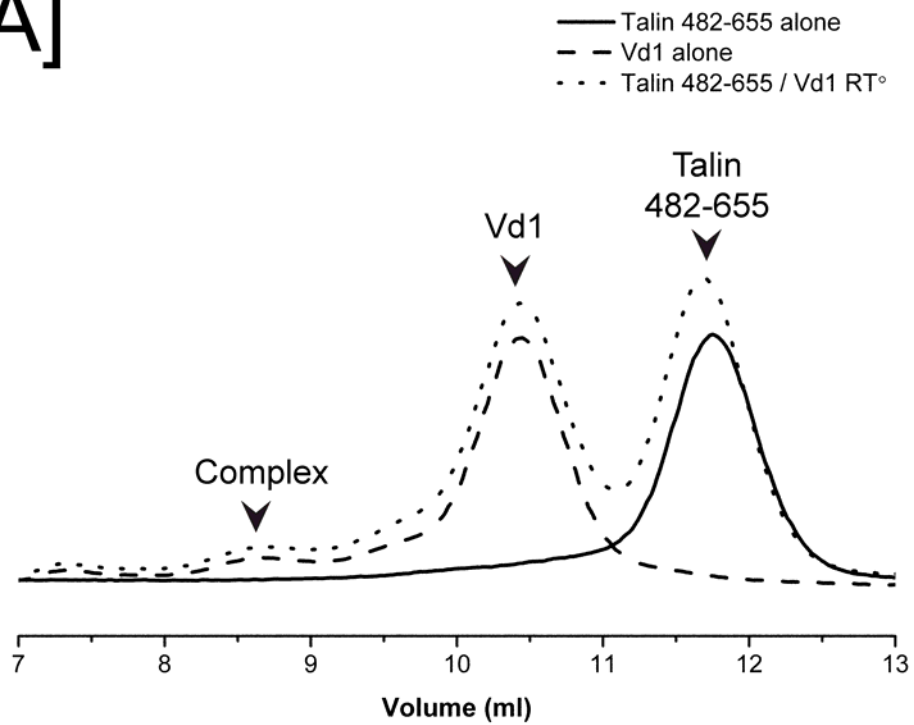


Figure 7

[A]



[B]

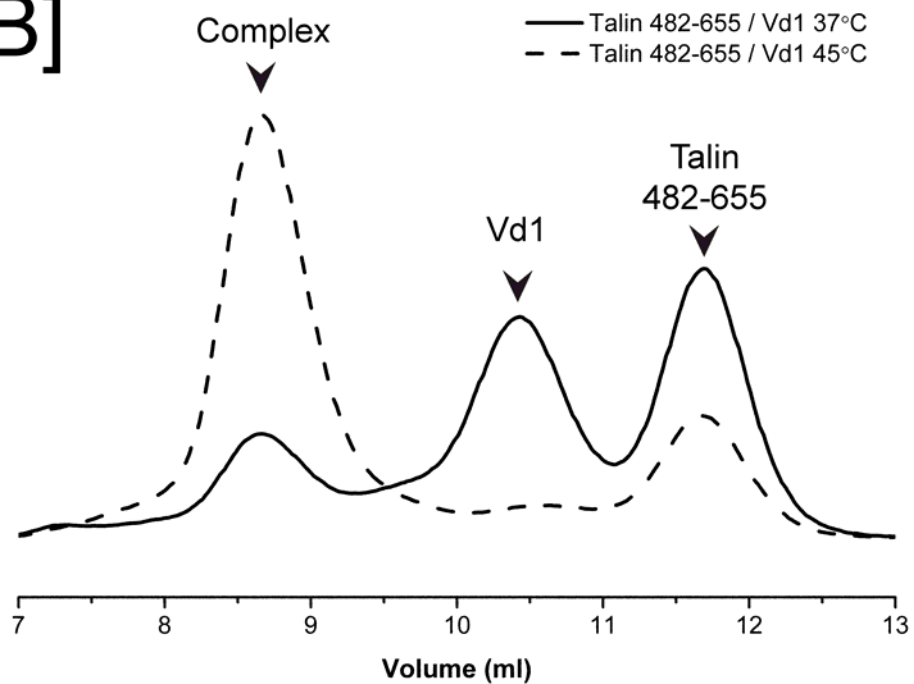


Figure 8

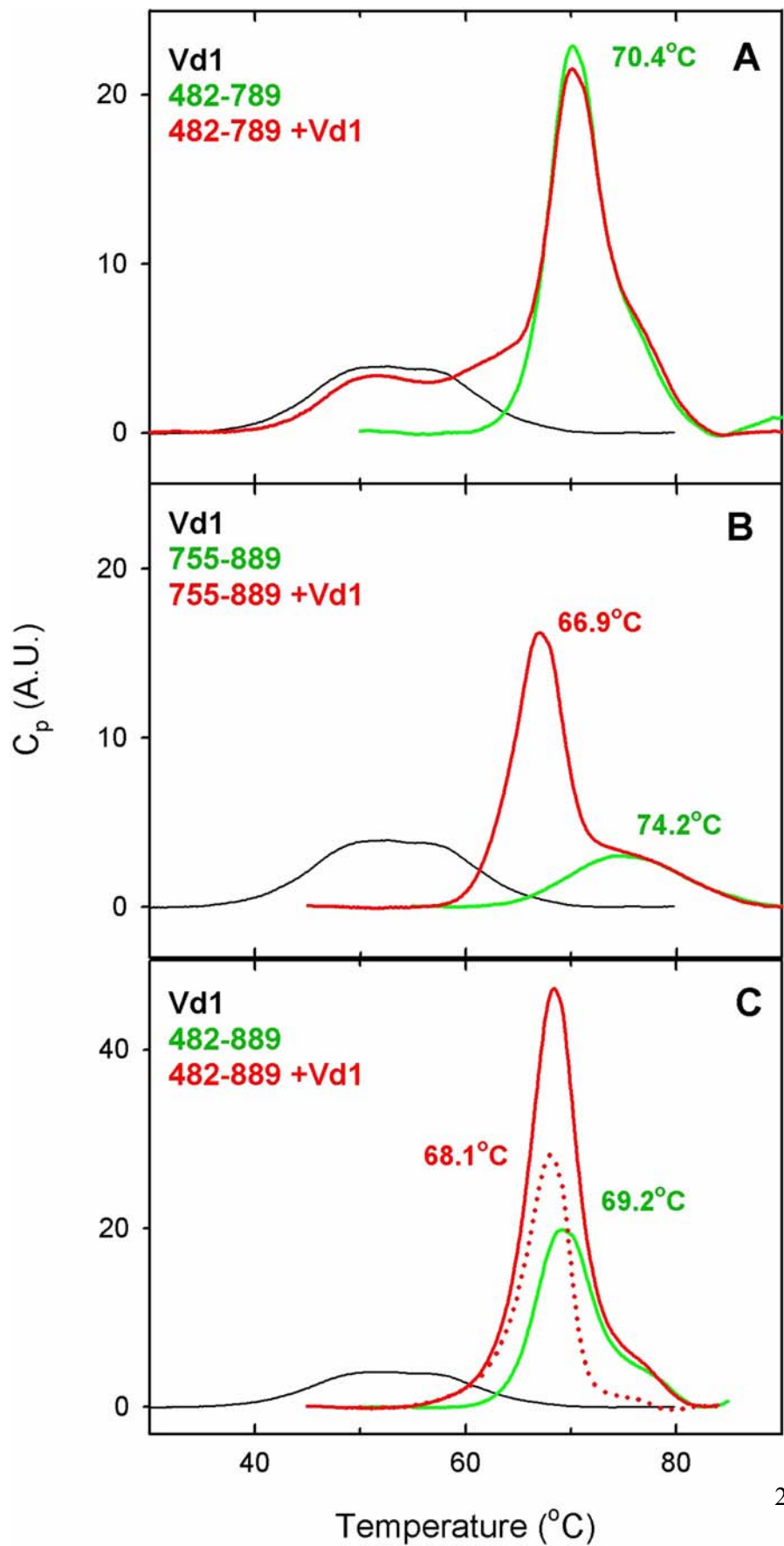


Figure 9

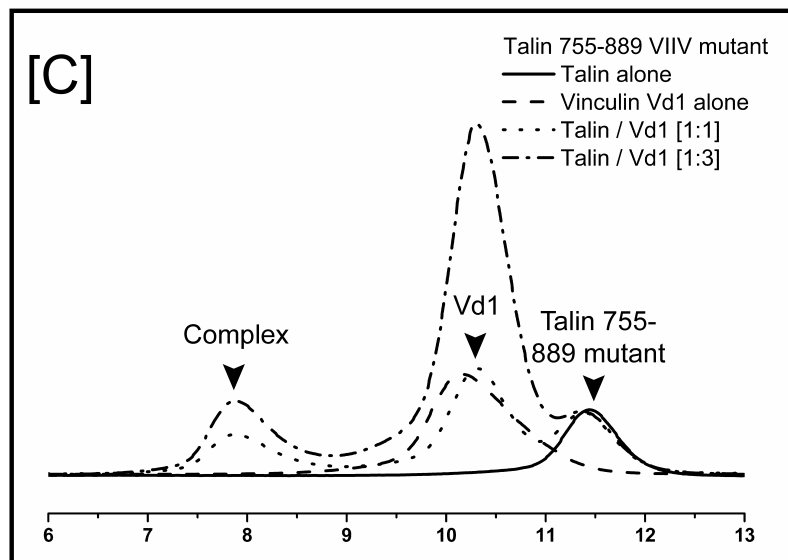
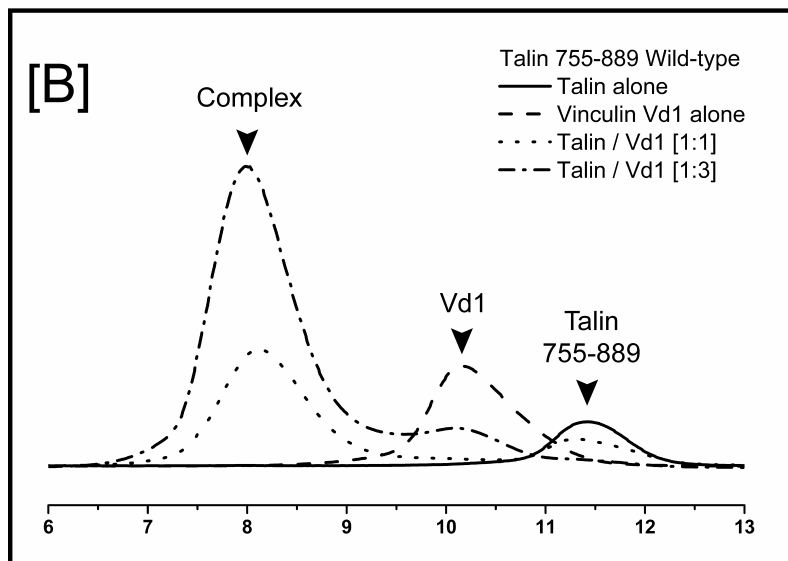
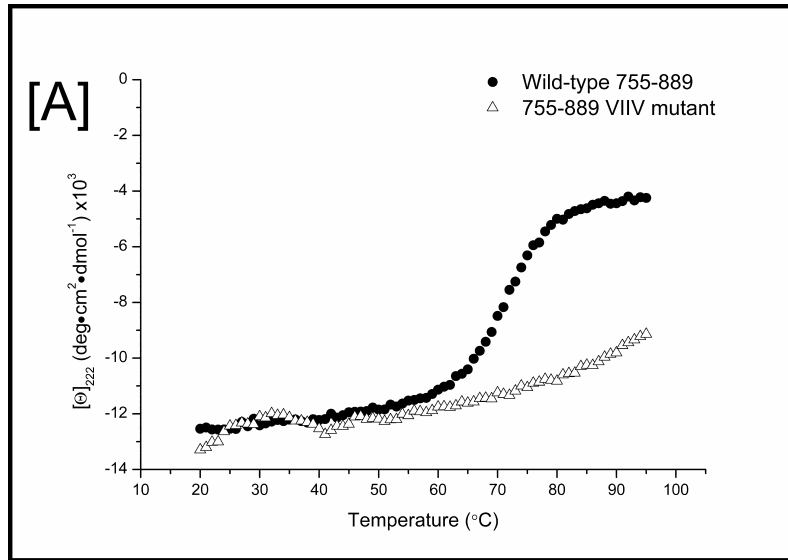


Figure 10

